Conductance Measurements of Nanoscale Regions with *in situ* Transmission Electron Microscopy

Masashi Arita[1, *], Ryusuke Hirose[2,3, **], Kouichi Hamada[1] and Yasuo Takahashi[1]

1 Graduate School of Information Science and Technology, Hokkaido University, Sapporo 060-0814, Japan

2 Graduate School of Engineering, Hokkaido University, Sapporo 060-0813, Japan

3 Research Fellow of the Japan Society for the Promotion of Science

* Corresponding author: Tel/Fax +81 11 706 6457, E-mail address arita@nano.ist.hokudai.ac.jp

** Present address: SII Nanotechnology Inc.

Abstract

Conductance measurements of nanostructures with simultaneous transmission electron microscopy (TEM) were performed on thin insulating SrF_2 films (3 nm thick) and Fe-SrF_2 granular films (10 nm thick) deposited on tip-shaped Au electrodes. By using a movable counter electrode, nanoscale regions were selected for investigation. Systematic measurements taken during the deformation of the SrF_2 film by the counter electrode provided a tunnelling barrier height of about 2.5 eV. The conductance of Fe-SrF_2 in nanoscale (~ 500 nm^2) showed the Coulomb-staircase-like characteristics at room temperature. The staircase period approximately corresponded to the value estimated from the geometry observed by TEM. The feasibility of this method is briefly described.

Key Words: transmission electron microscopy, scanning tunnelling spectroscopy, SrF_2, Fe-SrF_2 granular film, Coulomb staircase

1. Introduction

In recent years, the conductance of nanostructures such as the tunnel magnetoresistance (TMR) [1], the single electron tunnelling (SET) [2] and the conductance quantization of nanowires [3] has been investigated Among them, researches to develop actual devices using the tunnelling effects and their integration are in progress and some devices are close to being on the market [1, 4]. The miniaturization of current paths by controlling the thickness of the tunnel barrier and reducing the size of the Coulomb islands to only a few nanometer plays a key role in the development of usable devices. Therefore, characteristic features of nanoparticle systems have been investigated [5, 6].

The tunnelling current of nanostructures is strongly influenced by their geometric arrangement. Scanning electron microscopy (SEM) is widely used to observe the Coulomb islands [5]. However, its spatial resolution is insufficient to observe the barrier widths of less than 1 nm. Scanning tunnelling microscopy (STM) provides a good resolution and makes it possible to investigate the electron charging effect of the Coulomb islands [7]. In this case, images cannot be observed during the electrical measurements such as the scanning tunnelling spectroscopy (STS). If *in situ* imaging of nanoscale regions were possible during the tunnelling measurements, important information for the design of nanodevices as well as for the nanometer scale physics is provided. With this in mind, combined TEM/STM experiments have been successfully performed to correlate the geometry and the electric properties of metallic nanowires [8-10] (TEM: transmission electron microscopy; even without the feedback

control, the word STM is used in this report). A similar experiment was carried out on metal-insulator granular films composed of metallic nanoparticles dispersed in an insulator matrix, and a clear Coulomb blockade effect was confirmed at room temperature (RT) when the contact area was small [11].

In the present work, the TEM/STM method was applied to insulating thin SrF_2 films and SrF_2/Fe-SrF_2 granular films. Using a movable tip-shaped electrode, nanoscale regions to be investigated were selected. The STS measurements and the simultaneous TEM observations were performed during deformation of these nano-regions, and the barrier height for the tunnelling conduction and the period of the Coulomb staircase were discussed by comparing them with the observed geometry.

2. Experiment

Three Au electrodes were set in a TEM, one of which was covered by the sample layer (i.e. SrF_2 or Fe-SrF_2). Here, the electrode covered by the sample is called the *Au-substrate* (or *Au-sub*) and the bare Au is called the *Au-tip*. The conduction properties of the nanoscale regions were measured between the Au-sub and one of the Au-tips.

A schematic drawing of the experimental system is shown in Fig. 1a. It is composed of a TEM, a custom-made TEM holder, a piezo controller, a stepping motor controller, a current-to-voltage converter, an STM measurement unit and a CCD camera system. The TEM

instrument was a JEM 200CX microscope evacuated using an oil diffusion pump with a liquid nitrogen trap placed near the sample. The vacuum was 10^{-4} - 10^{-5} Pa. The observations were performed at 200 kV. The TEM holder is shown in Fig. 1b. The fundamental design is same as the designs of those developed for studies on metallic nanowires [10, 12]. The holder is loaded with three mechanical micrometers for a coarse Au-tips movement (μm - mm) and a tube-type piezoactuator for a fine Au-tips movement (nm - μm) which is controlled by the piezo controller with the output voltage of ± 100 V. By using the stepping motor controller, a motor installed in this holder can be rotated, and one of the two Au-tips were selected for the experiment without breaking the vacuum [11]. The current between Au electrodes were measured by using the current-to-voltage converter and the STM measurement unit. During the experiments, the sample and the electrodes were exposed to an electron beam that generated a background current of a few nA. Because the net tunnel current was on the order of nA, the instability of the electron beam produced a fatal background noise. This was due to a stray field of about 4 μT from the TV monitor, the vacuum monitor and the TEM diffusion pump. Therefore, all these apparatus were switched off or placed far from the TEM during the observation. As a result, the field was reduced to about 0.06 μT and the background noise was lowered to be around 70 pA. This value was acceptable for the present experiments. The geometry of the sample layer were dynamically recorded by the CCD camera system.

The electrodes having sharp apexes (Au-tips and Au-subs) were prepared from Au wires or

Au plates (purity: 99.95%) by an ion sputtering method using diamond or graphite powders as the mask material (the *ion-shadow method* [13, 14]). The radius of curvature of the apex was usually about 20 nm or less. After the fabrication of needle-shaped apex, the electrodes were washed using acetone and methanol in an ultrasonic bath. They were annealed at 420 K for 30 minutes and used as substrates for deposition. The samples to be measured were the SrF_2 single layer and the Fe-SrF_2 composite layer deposited on the Au-subs. Deposition was performed by electron beam evaporation of metallic Fe ingots (99.95%) and sintered SrF_2 tablets (99.9%). The vacuum during deposition was about 10^{-6} Pa. By moving the Au-tip so that it lightly touched the sample, the tunnelling current was measured during the simultaneous TEM observation. Each current-voltage (*I*-*V*) curve was obtained for 7 ms and no data averaging was performed.

3. Results and Discussion

3.1 Barrier height of SrF_2

A SrF_2 layer having a thickness of 3 nm was deposited on the Au-sub at a rate of 0.05 nm/s and its barrier height for the tunnel conduction was evaluated. The result is shown in Fig. 2. First, the Au-tip was gently contacted the SrF_2 surface (Fig. 2a). The insulating width was 3 nm and the contact area was about 200 nm^2. This contact area was estimated by assuming a circular contact having a diameter measured in Fig. 2a. In this case, the current through the

SrF_2 layer was too small to be detected by this system because the barrier width was large. Afterwards, the tip was pressed to reduce the barrier width by deformation (Fig. 2b). The barrier width and the contact area estimated using this TEM image were about 1 nm and about 200 nm^2, respectively. The *I-V* curve showed nonlinear characteristics as seen in Fig. 2c. The current was 0.13 nA at V_b = 0.1 V (V_b : bias voltage). Further pressure decreased the barrier width to 0.6 nm and increased the contact area to 300 nm^2 (Fig. 2d). This yielded a larger current flow of 10 nA at V_b = 0.1 V (Fig. 2e).

Although the electrode surfaces were curved, the radius of curvature at the apex was much larger than the contact size. Therefore, the SrF_2 layer was assumed to be sandwiched by two planar electrodes. In such a case, the Simmons' equation [15] can be used to analyse the *I-V* curves.

$$I = \frac{S}{t}\cdot\left(\frac{e}{h}\right)^2 \cdot \sqrt{2m\phi}\cdot \exp\left(-D\sqrt{\phi}\right)\times\left\{V_b + \left(\frac{D^2e^2}{96\phi} - \frac{De_2}{32\phi\sqrt{\phi}}\right)V_b{}^3\right\} \quad (1)$$

$$D = 4\pi t\cdot\frac{\sqrt{2m}}{h} \quad (2)$$

Here, I is the current, S is the contact area, t is the barrier width, ϕ is the barrier height and V_b is the bias voltage. The constants e, m and h are the electron charge, the electron mass and the Planck's constant, respectively. By selecting units of I, S, t , ϕ and V_b as nA, nm^2, nm, eV and V, respectively, the equation is described as follows.

$$I = S\times 3.159\times 10^4\,\frac{\sqrt{\phi}}{t}\exp\left(-10.246\,t\sqrt{\phi}\right)\times\left\{V_b + \left(1.0936\frac{t^2}{\phi} - 0.3202\frac{t}{\phi\sqrt{\phi}}\right)V_b{}^3\right\} \quad (3)$$

Least-square fitting analyses were performed using Eq. (3) by assuming the contact areas observed in TEM images, i.e. $S \sim 200$ nm^2 for Fig. 2d and $S \sim 300$ nm^2 for Fig. 2e. As the result, $\phi \sim 2.5$ eV and $t \sim 1.0$ nm for Fig. 2d and $\phi \sim 2.5$ eV and $t \sim 0.8$ nm for Fig. 2e were obtained. The estimated barrier widths are almost the same as the values obtained from TEM images. The barrier height values for Figs. 2d and 2e are the same each other. The energy gap of SrF_2 is known to be larger (11.25 eV) than oxides such as MgO and the resistance of Fe-SrF_2 granular films was reported to be much larger than that of Fe-MgO [16]. Therefore, the values obtained in this work are reasonable.

3.2 Coulomb staircase of Fe-SrF_2 granular film

On the Au-sub, a 10 nm thick Fe-SrF_2 granular film (*ca*. 37vol% Fe) was deposited at RT by co-evaporation of Fe and SrF_2. In this case, the Fe particles were about 3 nm in diameter. Considering the film thickness and the particle size, 2 - 3 nanoparticles were though to be arranged in series along the thickness and they form a multi-barrier tunnelling path. Afterwards, a thin SrF_2 layer (1 nm thick) was deposited. This procedure is for an introduction of an inhomogeneous resistance configuration along the film thickness to enhance the Coulomb staircase effect.

The results of the sample measurements on the Au-sub are presented in Fig. 3 where the TEM images captured using a CCD camera and *I*-*V* curves are compared. First, the Au-tip

lightly pressed the granular film as in Fig. 3a. In this case, the Au-tip was slightly deformed. The contact area was about 560 nm^2. In this area, there were about 30 - 40 nano particles. The corresponding *I-V* curve shows the nonlinear properties characteristic of tunnelling conduction. Next, the Au-tip was moved slowly in the direction indicated by the white arrow in Fig. 3b to reduce the contact area and the *I-V* curves were measured (Figs. 3b - 3h). By reducing the contact area, the current was monotonically reduced. The currents at V_b = 1 V were 0.26, 0.21, 0.16 and 0.13 nA for Figs. 2b, 2d, 2f and 2h, respectively. The measurements were carried out at several places and were quite similar results to those in Fig. 3. Compared with our earlier work using a 40 nm thick Fe-SrF_2 (~ 37 vol% Fe) without the SrF_2 top layer [11], the current in this work is about one order smaller. This is thought to be due to the existence of the 1 nm thick SrF_2 top layer. Because the current is small, the Coulomb blockade could not be identified in these *I-V* curves. Assuming that three nanoparticles are in series along the thickness, the total capacitance is estimated as C_Σ = 0.43 aF. Thus, the threshold voltage for the Coulomb blockade is $V_{th} = e/2C_\Sigma$ = 0.2 V where *e* is the electron charge. The current at V_b = 0.2V is about 30 pA as seen in Fig. 3h. This current value is less than the resolution limit of the measurement system used here. This is likely a reason that detecting the Coulomb blockade was difficult.

By focusing on Fig. 3d, weak steps are lying on the nonlinear curve. For clarification, the differential conductance curve is shown in Fig. 4. Peaks at V_b = - 2.0 V, -2.4 V and - 2.8 V can

be recognized. These peaks are due to the steps in the *I-V* curve that correspond to the Coulomb staircase. The staircase period was about 0.4 V as seen in Fig. 4b. While plural nanoparticles may form tunnel junctions in series along the layer thickness as described above, only the capacitance of the junction with the largest resistance contributes to the period of the Coulomb staircase. Therefore, the capacitance of the Fe nanoparticle facing to the SrF_2 top layer is important. Because the particles are sandwiched by two electrodes, the capacitance C is assumed to be half of the self-capacitance of a particle $C_s = 4\pi\varepsilon_0\varepsilon_r r$ (ε_0 and ε_r: dielectric constants of the vacuum and SrF_2, respectively, r: radius of the particle). By using the values $2r = 3$ nm and $\varepsilon_r = 7.69$ [17], the self-capacitance is $C_s = 1.3$ aF and the period is $e/C = 2e/C_s = 0.25$ V. This value approximately fits to the experimental result.

4. Summary and Conclusion

The characteristic feature of the TEM/STM method used here is that the geometrical observations with a spatial resolution of less than 1 nm, the selection and the deformation of nano structures and the conductance measurements can be performed simultaneously. This cannot be carried out by the other method available. In this report, two STS experiments are demonstrated. For a SrF_2 tunnel barrier, a conductance change during the deformation was detected and the barrier height of 2.5 eV was analysed. For a Fe-SrF_2 granular film covered by a SrF_2 layer, the Coulomb staircase was observed for a period of 0.4 V. These values are

valid compared with the theoretically expected values.

With the requirement of electronic devices in nanometer scale, qualified insulating materials have been explored for capacitors and tunnel barriers. Besides oxides such as SiO_2, Al_2O_3 and MgO, fluorides (e.g. CaF_2, SrF_2 and MgF_2) are also candidates to be used [18-20]. In present, the production of atomically smooth fluoride layer is difficult [18]. Considering the tunnel junctions in micrometer scale, the inhomogeneous layer thickness hinders the homogeneous current path and the barrier height is incorrectly estimated. In order to prevent this incorrect estimation, measurements of very tiny junctions are required. The TEM/STM method used here makes it possible. The value ϕ = 2.5 eV obtained in this work is thought to be a useful data. On the other hand, the granular films composed of ferromagnetic metallic nano-particles and fluoride have been reported to show a large TMR effect compared to the oxide systems [19,20]. Because the size of metal particles was a few nm, the SET effect is expected in addition the TMR effect. This report clearly demonstrated the SET effect of this system during the deformation. The results in this basic research will serve useful information to the future development of magnetic nano-devices.

Acknowledgements

This work was supported by a Grants-in-Aid from the Japan Society for the Promotion of Science (Nos. 587, 13650708, 16206038 and 17201029), The Murata Science Foundation,

Izumi Science and Technology Foundation, for which we are sincerely grateful.

References

1 E. Hirota, H. Sakakima, and K. Inomata, Giant Magneto-Resistance Devices, Springer, Berlin, 2002, references therein.

2 Y. Takahashi, Y. Ono, A. Fujiwara, and H. Inokawa, J. Phys.: Condens. Matter. 14 (2002) 995, references therein.

3 N. Agraït, A. L. Yeyati, and J. M. van Ruitenbeek, Phys. Rept. **377** (2003) 81, references therein.

4 S. Yuasa, T. Nagahama, A. Fukushima, Y. Suzuki, and K. Ando, Nature Mater. **3** (2004) 868.

5 E. M. Ford, and C. Dekker, and G. Schmid, Appl. Phys. Lett. **75** (1999) 421.

6 K. Yakushiji, S. Mitani, K. Takanashi, S. Takahashi, S. Mekawa, H. Imamura, and H. Fujimori, Appl. Phys. Lett. **78** (2001) 515.

7 B. Uri, C. Yunwei, K. David, and M. Oded, Nature **400** (1999) 542.

8 H. Ohnishi, Y. Kondo, and K. Takayanagi, Nature **395** (1998) 780.

9 T. Kizuka, S. Umehara, and S. Fujiwara, Jpn. J. Appl. Phys. Pt. 2 **40** (2001) L71.

10 M. Arita, T. Tajiri, K. Hamada, and H. Miyagi, J. Magn. Soc. Jpn. **29** (2005) 120.

11 R. Hirose, M. Arita, K. Hamada, Y. Takahashi, and A. Subagyo, Jpn. J. Appl. Phys. Pt. 2 **44** (2005) L790.

12 T. Kizuka, K. Yamada, S. Deguchi, M. Naruse, and N. Tanaka, Phys. Rev. B **55** (1997) 7398.

13 M. Arita, R. Takei, M. Yoshida, K. Hamada, A. Okada, K. Mukasa, and H. Takahashi, Int. J. Jpn. Soc. Prec. Eng. **33**, 215 (1999).

14 R. Hirose, M. Arita, K. Hamada, and A. Okada, Mater. Sci. Eng. C **23** (2003) 927.

15 J. G. Simmons, J. Appl. Phys. **34** (1963) 1793.

16 H. Hosoya, Master Thesis, Hokkaido Univ., Sapporo, 2003.

17 H. P. R. Frederikse and J. C. Slater: in D. E. Gray (Ed), American Institute of Physics Handbook, Sec. 9c, McGraw-Hill, New York, 3rd ed.,1972, p. 9-112.

18 T. Asano, H. Ishikawa and N. Kaifu, Jpn. J. Appl. Phys. **22** (1983) 1474.

19 T. Furubayashi and I. Nakatani: J. Appl. Phys. **79** (1996) 6258.

20 N. Kobayash, S. Ohnuma, T. Masumoto and H. Fujimori: J. Appl. Phys. **90** (2001) 4159.

Figure Captions

Fig. 1 (a) Schematic drawing of the experimental system. (b) The custom-made TEM holder. The electrodes are placed in the hole at the top of the holder bar.

Fig. 2 (a), (b) and (d) TEM images captured using a CCD camera during deformation of SrF_2 by the Au-tip. The numbers in the bottom-right corners are the contact areas. The Au-tip was pressed along the direction indicated by arrows in (b) and (d). (c) and (e) The *I-V* curves indicating the tunnel conduction that correspond to (b) and (d), respectively.

Fig. 3 TEM images and I-V curves during the change of contact areas. The Au-tip was moved along the direction indicated by the arrow in (c). The numbers in the bottom-right corners of the images are the contact areas. The image and the graph in the same line correspond to each other.

Fig. 4 (a) *I-V* curve and (b) differential conductance curve of Fig. 3d. Peaks in (b) marked by arrows correspond to faint steps in (a) which are thought to be the Coulomb staircase.

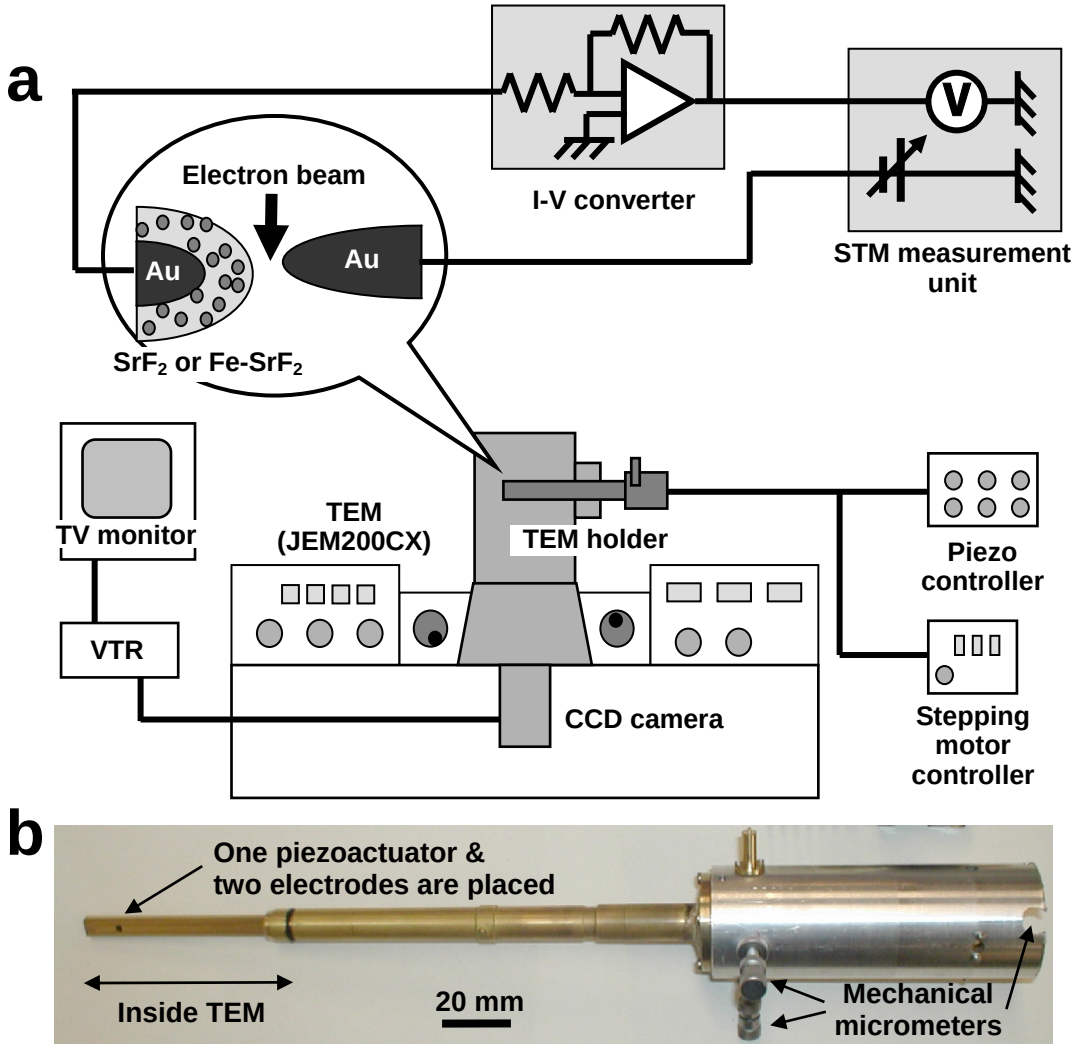

Fig. 1 Conductance Measurements of Nanoscale Regions with *in situ* Transmission Electron Microscopy (Arita et al.)

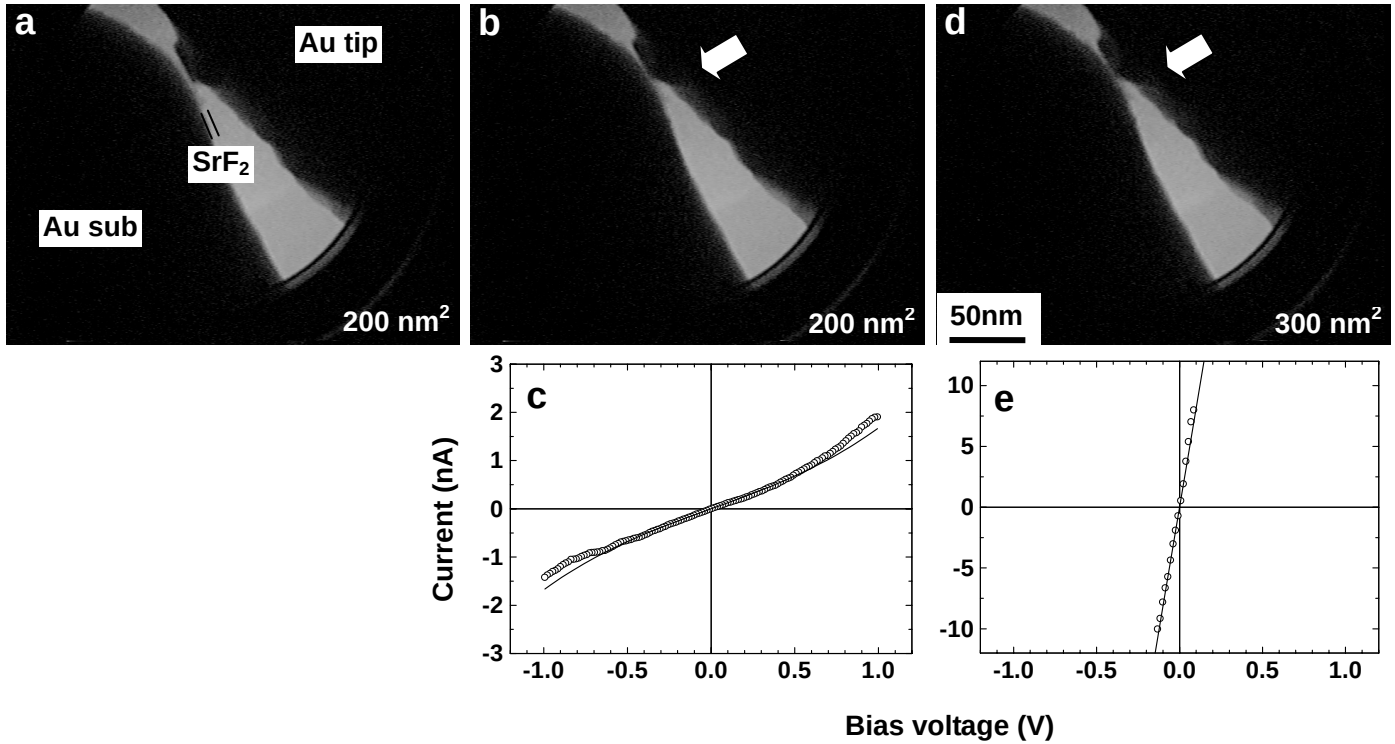

Fig. 2 Conductance Measurements of Nanoscale Regions with *in situ* Transmission Electron Microscopy (Arita et al.)

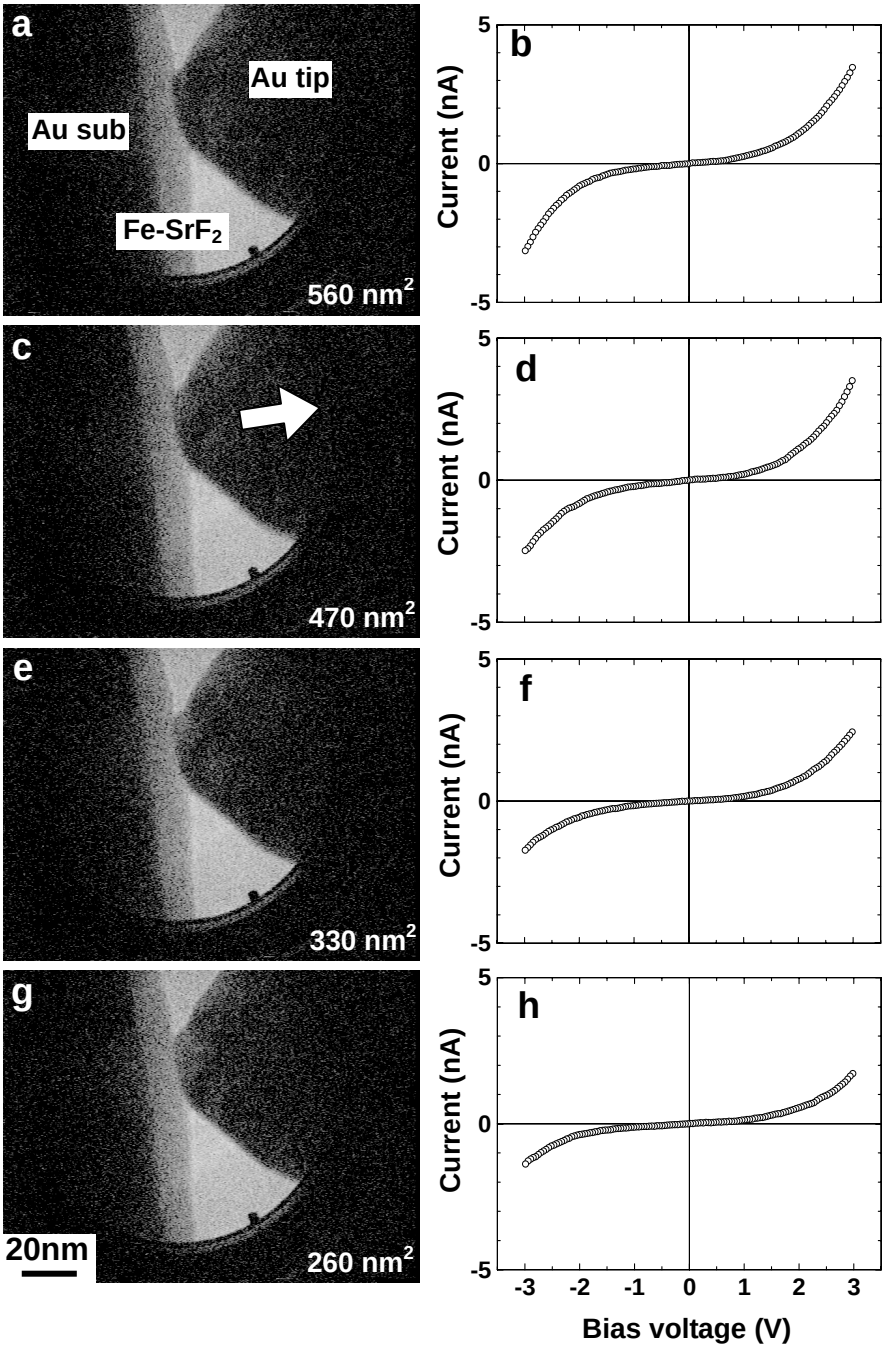

Fig. 3 Conductance Measurements of Nanoscale Regions with *in situ* Transmission Electron Microscopy (Arita et al.)

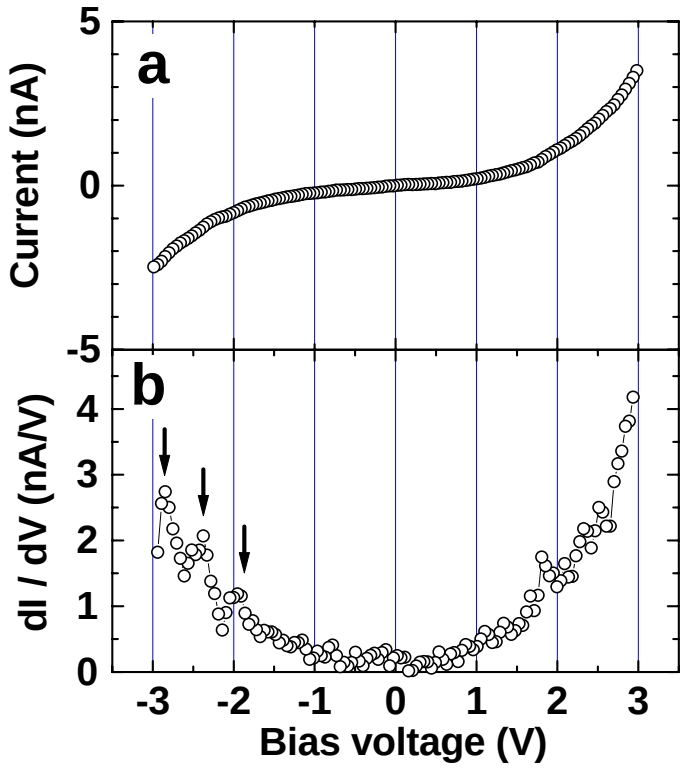

Fig. 4 Conductance Measurements of Nanoscale Regions with *in situ* Transmission Electron Microscopy (Arita et al.)